Molecular Therapy
Oncolytics
Original Article

Trap and ambush therapy using sequential primary and tumor escape-selective oncolytic viruses

Mason J. Webb,[1,2,10] Timothy Kottke,[2,10] Benjamin L. Kendall,[2] Jack Swanson,[3] Chisom Uzendu,[2] Jason Tonne,[2] Jill Thompson,[2] Muriel Metko,[2] Madelyn Moore,[2] Mitesh Borad,[4] Lewis Roberts,[5] Rosa M. Diaz,[2] Michael Olin,[6] Antonella Borgatti,[7,8,9] and Richard Vile[2,3]

[1]Division of Hematology/Medical Oncology, Mayo Clinic, Rochester, MN 55905, USA; [2]Department of Molecular Medicine, Mayo Clinic, Rochester, MN 55905, USA; [3]Department of Immunology, Mayo Clinic, Rochester, MN 55905, USA; [4]Division of Hematology/Oncology, Mayo Clinic, Scottsdale, AZ 85259, USA; [5]Division of Gastroenterology and Hepatology, Mayo Clinic, Rochester, MN 55905, USA; [6]Division of Pediatric Hematology and Oncology, University of Minnesota, Minneapolis, MN 55455, USA; [7]Department of Veterinary Clinical Sciences, University of Minnesota, St. Paul, MN 55108, USA; [8]Masonic Cancer Center, University of Minnesota, Minneapolis, MN 55455, USA; [9]Clinical Investigation Center, University of Minnesota, St. Paul, MN 55108, USA

In multiple models of oncolytic virotherapy, it is common to see an early anti-tumor response followed by recurrence. We have previously shown that frontline treatment with oncolytic VSV-IFN-β induces APOBEC proteins, promoting the selection of specific mutations that allow tumor escape. Of these mutations in B16 melanoma escape (ESC) cells, a C-T point mutation in the cold shock domain-containing E1 (*CSDE1*) gene was present at the highest frequency, which could be used to ambush ESC cells by vaccination with the mutant CSDE1 expressed within the virus. Here, we show that the evolution of viral ESC tumor cells harboring the escape-promoting *CSDE1*$^{C\text{-}T}$ mutation can also be exploited by a virological ambush. By sequential delivery of two oncolytic VSVs *in vivo*, tumors which would otherwise escape VSV-IFN-β oncolytic virotherapy could be cured. This also facilitated the priming of anti-tumor T cell responses, which could be further exploited using immune checkpoint blockade with the CD200 activation receptor ligand (CD200AR-L) peptide. Our findings here are significant in that they offer the possibility to develop oncolytic viruses as highly specific, escape-targeting viro-immunotherapeutic agents to be used in conjunction with recurrence of tumors following multiple different types of frontline cancer therapies.

INTRODUCTION

A major challenge for the development of effective cancer therapies is that tumors are genetically neither homogeneous nor static and typically evolve very rapidly in response to applied treatment.[1–3] Thus, initial robust responses to therapy are frequently followed by aggressive recurrence as treatment-resistant clones are selected from the ongoing mutational pool, leading to progressive disease that is both phenotypically and genetically distinct from the initial malignancy.[4–11] One mechanism that drives cancer plasticity is the action of APOBEC proteins (apolipoprotein B mRNA editing enzyme, catalytic polypeptide-like), a broad family of cytosine deaminases that protect from viral infection in healthy mammals. APOBEC family proteins have been previously shown to drive mutagenesis in cancer cells and contribute to escape in response to multiple types of therapy.[1,9,10]

In this respect, we have previously shown that APOBEC-mediated mutagenesis is a major driver of resistance to oncolytic virotherapy with the vesicular stomatitis virus (VSV).[9] Replication of VSV, a single-strand negative sense RNA virus (rhabdovirus, Indiana serotype), is highly sensitive to inhibition by interferon (IFN). In our prior work to enhance safety of this virus, we overexpressed the IFN-β gene with the goal of selective replication in type I IFN-defective tumor cells and rapid inhibition in normal, IFN-responsive cells.[12–16] This viral platform has been tested clinically (NCT03120624, NCT03865212, and NCT03647163). Using *in vitro* and *in vivo* models, we showed that infection of tumors with VSV-IFN-β induced type I IFN-dependent human APOBEC3B- or murine APOBEC3-, which induced mutations of the target tumor cell genome that were associated directly with escape of virus/oncolysis-resistant (VSV-ESC) cells.[8,9] Whole-genome sequencing of these VSV-ESC cells identified reproducible mutational signatures associated with escape, the most predominant of which was a C-T mutation in the cold shock domain-containing E1 (CSDE1) gene (*CSDE1*$^{C\text{-}T}$), which converts a proline to serine at αα5 (CSDE1^{P5S}).[9,10] CSDE1, a multi-functional RNA binding protein that regulates RNA translation and turnover,[17–19] stimulates cap-independent translation initiation for several viruses,[20] and serves as an RNA chaperone bridging viral RNAs and proteins that cannot bind directly to each other. We went on to show that CSDE1 is a critical mediator

Received 9 January 2023; accepted 18 May 2023;
https://doi.org/10.1016/j.omto.2023.05.006.

[10]These authors contributed equally

Correspondence: Richard G. Vile, PhD, Mayo Clinic, Guggenheim 18, 200 1st St SW, Rochester, MN 55905, USA.
E-mail: vile.richard@mayo.edu

This is an open access article under the CC BY-NC-ND license (http://creativecommons.org/licenses/by-nc-nd/4.0/).

of VSV replication and that the *CSDE1*$^{C\text{-}T}$ mutation in target tumor cells is a predictable and reproducible mechanism of cellular escape from viral lysis. Therefore, cumulatively our data have shown that APOBEC-induced mutations rapidly allow for selection of tumor cells that have acquired a few highly predictable and reproducible mutations that serve to decrease viral fitness and, therefore, reduce viral replication and oncolysis in escaping tumor cells.[9,21]

Since CSDE1^{WT} is an important mediator of VSV replication, we constructed a modified version of VSV-IFN-β in which the *CSDE1* gene is co-expressed between the viral *G* and *L* genes. By providing additional levels of CSDE1 in infected cells, this VSV-IFN-β-CSDE1 virus replicated to higher levels than the parental VSV-IFN-β virus and was a significantly more potent oncolytic *in vivo*, especially when used in combination with late administered anti-PD-1 antibody immune checkpoint blockade (ICB).[21] We also immunotherapeutically exploited the *in vivo* generation of the mutant CSDE1^{P5S} protein in escape tumor cells as an escape-associated tumor antigen (EATA), by "ambushing" tumors that escaped VSV-IFN-β treatment through vaccination against EATA encoded within the virus itself.[21]

Just as tumors evolve to escape VSV oncolytic therapy (such as by loss of function, through mutation, of CSDE1), we observed that VSV can co-evolve to complement tumor-specific mutations such as *CSDE1*$^{C\text{-}T}$, although viral adaptation lags behind tumor evolution, contributing to treatment failure. With prolonged culture of VSV in *CSDE1*$^{C\text{-}T}$ mutated cells, we observed the emergence of a predominant viral variant containing a single C-U mutation within the only perfect CSDE1 consensus binding site within the VSV genome at the intergenic region (IGR) between the *P* and *M* genes.[21] This P/M^{C-U} viral mutation complemented the host cell *CSDE1*$^{C\text{-}T}$ mutation, allowing near wild-type levels of replication of the VSV-IFN-β-P/M virus in escaped *CSDE1*$^{C\text{-}T}$ tumor cells. Taken together, our preliminary studies showed that (1) the escape-associated mutant CSDE1^{P5S} protein decreases viral replication fitness, and, therefore, promotes tumor cell escape from oncolysis by interfering with the ability of the CSDE1 protein to interact with the IGR between the *P* and *M* genes of VSV-IFN-β,[21] (2) by expressing CSDE1^{WT} in the virus, these additional levels of CSDE1 allow for better replication and oncolysis compared with the parental VSV-IFN-β, and (3) the VSV-IFN-β-P/M virus compensates for the *CSDE1*$^{C\text{-}T}$ mutation, allowing high-level replication and oncolysis in cells that have escaped oncolysis by wild-type VSV-IFN-β.

Here, we test the hypothesis that, in response to VSV-IFN-β oncolytic therapy, neoplastic cells that escape do so predominantly by genetically fixing a predictable mutation C-T mutation in the *CSDE1* gene; however, this makes them vulnerable to infection by the highly escape-specific oncolytic VSV-IFN-β-P/M virus. Our data show that the initial response to VSV-mediated oncolytic virotherapy can be significantly improved using the second-generation VSV-IFN-β-CSDE1 oncolytic virus. Furthermore, by introducing sequential viral treatments starting with VSV-IFN-β-CSDE1 then subsequently treating with the escape-selective VSV-IFN-β-P/M virus, we enhanced the numbers of complete tumor cures generated compared with treatment with the parental VSV-IFN-β or VSV-IFN-β-CSDE1 virus alone. We also show that the therapeutic benefits of combination of oncolytic VSV-IFN-β-CSDE1 with VSV-IFN-β-P/M led to immune effectors, the efficacy of which could be further enhanced by ICB. Overall, our data are noteworthy because they show that, in addition to an immunological trap (VSV treatment) and ambush (vaccination with the escape-associated CSDE1^{P5S} EATA),[21] it is possible to use an oncolytic trap and ambush strategy to target initial treatment failure with a highly targeted, escape-selective oncolytic virus—and that the immunotherapeutic sequelae of improved oncolytic therapy can be further exploited with ICB.

RESULTS

VSV-IFN-β-CSDE1 has enhanced replication and cytotoxicity compared with VSV-IFN-β

We have previously shown that tumor cells escape VSV-IFN-β-mediated oncolysis by fixing at high frequency the APOBEC-induced *CSDE1*$^{C\text{-}T}$ mutation,[21] revealing a critical role for CSDE1 in the replication of VSV. CSDE1, an RNA-binding protein involved in translational control, binds at the consensus site 5′-(purine) (aagua)-3′.[17–19,22–26] This exact consensus site is present in the IGR of VSV between the *P* and *M* genes during replication of the VSV genome when the positive sense strand is generated.[21] Consistent with the hypothesis that enhanced levels of virus-expressed CSDE1^{WT} protein would therefore enhance viral replication, we confirmed that the second-generation oncolytic VSV-IFN-β-CSDE1 replicated significantly more efficiently than the parental first-generation VSV-IFN-β in wild-type tumor cells (Figure 1A). Conversely, the VSV-IFN-β-P/M virus containing a single C-U mutation in the P/M IGR, isolated by serial passage through tumor cells that had escaped VSV-IFN-β oncolysis and which express the mutant CSDE1^{P5S} protein, replicated 2–3 orders of magnitude less efficiently than VSV-IFN-β (Figure 1A). Similarly, whereas VSV-IFN-β-CSDE1 was more cytotoxic to wild-type tumor cells than VSV-IFN-β over a 72-h time course, VSV-IFN-β-P/M showed minimal cytotoxicity (Figure 1B). When tumor cells were exposed to low multiplicity of infection (MOI) with VSV-IFN-β for 21 days, VSV-ESC cells could be isolated (Figure 1C), in which the *CSDE1*$^{C\text{-}T}$ mutation occurs at very high frequency (>90% by Sanger sequencing).[9,21] In contrast, long-term exposure of wild-type tumor cells to VSV-IFN-β-CSDE1 led to significantly decreased amounts of escape (fewer surviving cells) (Figure 1C). These data show that increasing the levels of CSDE1^{WT} from the virus both increased viral replication and oncolysis and significantly reduced the possibility of target cell escape. Interestingly, 21-day exposure of wild-type tumor cells to VSV-IFN-β-P/M led to significantly fewer escaped surviving cells than did VSV-IFN-β (Figure 1C); we hypothesize that this effect is attributable to the low levels of replication maintained by VSV-IFN-β-P/M against wild-type tumor cells (Figure 1B) leading to the selection of CSDE1^{P5S} mutant ESC cells, which then provide a substrate for replication of the VSV-IFN-β-P/M virus in the cultures.

CSDE1 mediates generation of unicistronic *M* and *P* RNA

VSV sequesters its replication machinery into specialized non-membrane-bound cytoplasmic compartments where RNA synthesis

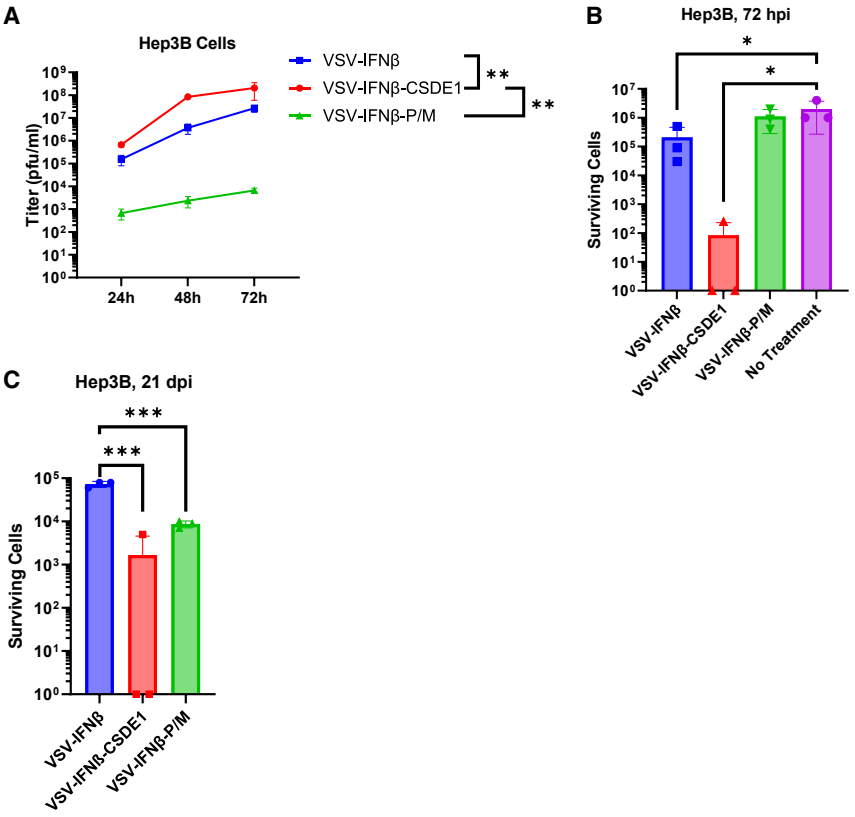

Figure 1. VSV-IFN-β-CSDE1 and VSV-IFN-β-P/M target virus sensitive and virus-escape tumor cells, respectively

Hep3B cells were infected in triplicate with VSV-IFN-β, VSV-IFN-β-CSDE1, or VSV-IFN-β-P/M (MOI = 0.1). (A) Viral titers (pfu/mL) were determined by plaque assay at 24, 48, and 72 h. Significance was determined by two-way ANOVA with interaction and repeated measures, mean ± SEM shown. (B) Number of surviving cells at 72 h post infection (hpi). (C) Hep3B tumor cells were exposed to low MOI with VSV-IFN-β, VSV-IFN-β-CSDE1, or VSV-IFN-β-P/M (MOI = 0.01) for 21 days and surviving VSV-ESC cells were counted (days post infection, dpi). All cell counts in (B and C) show means of triplicate wells with individual data points shown. Significance for (B and C) was calculated using one-way ANOVA, pairwise comparisons using t tests with pooled standard deviation. Statistical significance: *$p < 0.05$, **$p < 0.01$, ***$p < 0.001$.

occurs.[27–30] Consistent with its role in the replication of VSV, we observed that CSDE1 also localized to cytoplasmic compartments in VSV-infected cells (Figures 2A and 2B). The C-U mutation in VSV-IFN-β-P/M, which greatly inhibits the ability of the virus to replicate in parental CSDE1^{WT} cells, occurs in the CSDE1 consensus binding site, which is in the viral genome at a single base within the IGR between the *P* and *M* genes (Figure 2C). Therefore, we tested the hypothesis that CSDE1 mediates viral replication through control of *P* and/or *M* gene expression. During normal VSV replication, unicistronic *P* and *M* mRNAs are made by disengagement of the viral polymerase at the *P-M* IGR (*P* mRNA) with subsequent re-initiation of transcription at the *M* gene (*M* mRNA). Failure of the polymerase to detach from the nascent *P* transcript would create a bicistronic *P-M* mRNA. qRT-PCR from tumor cells infected with VSV-IFN-β, VSV-IFN-β-CSDE1^{WT}, or VSV-IFN-β-P/M showed that there was no significant difference in *P* mRNA expression between any of these viruses (Figure 2C). However, a 3-fold increase in *M* mRNA expression was observed in cells infected with VSV-IFN-β-CSDE1^{WT} compared with VSV-IFN-β (Figure 2D), consistent with the significantly enhanced replication capacity of VSV-IFN-β-CSDE1 over VSV-IFN-β (Figure 1). In contrast, infection with VSV-IFN-β-P/M led to dramatically reduced levels of *M* mRNA expression (Figure 2D), also consistent with the inability of this virus to replicate well in normal CSDE1^{WT} cells (Figure 1). Although levels of bicistronic *P-M* RNA were largely undetectable in cells infected with VSV-IFN-β or VSV-IFN-β-CSDE1 (Figure 2E), there were significant levels of bicistronic *P-M* mRNA in cells infected with VSV-IFN-β-P/M with greater than a 100-fold increase when compared with the VSV-IFN-β control (Figure 2E).

Consistent with the qRT-PCR data, tumor cells infected with VSV-IFN-β-P/M produced very low levels of M protein (Figure 2F, lane 3) as would be expected from a bicistronic mRNA with the *M* gene in the downstream position. Conversely, infection with VSV-IFN-β-CSDE1^{WT} enhanced M protein expression compared with VSV-IFN-β (Figure 2F, lanes 1 and 2). This pattern of M protein expression was completely reversed following infection of ESC, *CSDE1*$^{C\text{-}T}$ mutant tumor cells previously selected for escape from VSV-IFN-β. Thus, infection of ESC cells with VSV-IFN-β yielded very low levels M protein (Figure 2F, lane 4)—consistent with an incompatibility of the wild-type consensus CSDE1 binding site (in VSV-IFN-β) with the mutant CSDE1^{P5S} protein (in the ESC cells). However, this effect was rescued by exogenous supply of the wild-type CSDE1 protein in the virus following infection with VSV-IFN-β-CSDE1 (Figure 2F, lane 5). Finally, infection of the ESC, *CSDE1*$^{C\text{-}T}$ mutant tumor cells with VSV-IFN-β-P/M generated wild-type levels of M protein (Figure 2F, lane 6) consistent with restoration of normal transcription of unicistronic *M* RNA through complementation of the CSDE1^{P5S} mutant protein in the ESC cells by the C-U mutation in the P/M IGR in the VSV-IFN-β-P/M virus.

We hypothesized that, under conditions where the host cell expressed CSDE1 status (CSDE1^{WT} or CSDE1^{P5S} mutant) is mismatched to the viral consensus CSDE1 binding site (P/M IGR wild-type or C-U mutant), the functionality of the viruses released would be severely impaired as reflected in the generation of increased levels of defective interfering particles (DIPs). In this respect, supernatants from CSDE1^{WT} tumor cells infected with VSV-IFN-β-P/M (CSDE1

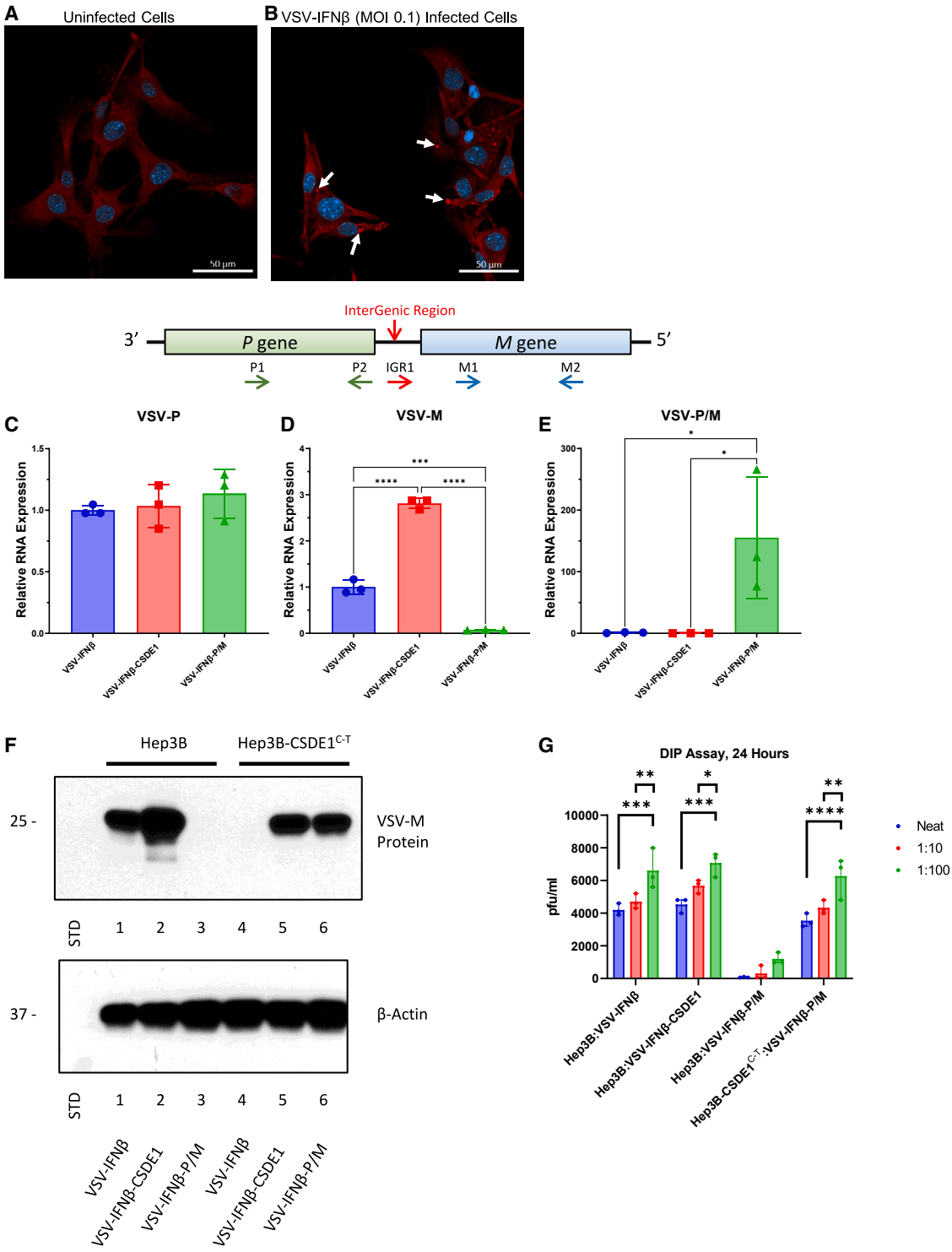

Figure 2. CSDE1 localizes to intracellular compartments in VSV-infected cells and regulates viral *P* and *M* RNA levels

Immunofluorescence for CSDE1 (red) and DAPI (blue) in (A) uninfected B16 parental cells and (B) B16 parental cells infected with VSV-IFN-β (MOI = 0.1) at 8 h post infection. Arrows show areas of cytoplasmic CSDE1 concentration resembling VSV replication compartments. Scale bars, 50 μm. (C–E) Hep3B cells were infected in triplicate wells with VSV-IFN-β, VSV-IFN-β-CSDE1, or VSV-IFN-β-P/M (MOI = 3.0). qRT-PCR from infected cells 6 h later is shown for (C) viral *P* (primers P1 and P2), (D) viral M (primers M1 and M2), or (E) bicistronic P/M RNA (primers IGR1 and M2). Significance for (C–E) was determined using one-way ANOVA. (F) Hep3B parental cells (lanes 1–3) or Hep3B cells

(legend continued on next page)

consensus binding site mutant) were more inhibitory against infection of BHK cells with a stock VSV than were supernatants harvested from infection of CSDE1^{WT} tumor cells with either VSV-IFN-β or VSV-IFN-β-CSDE1^{WT} (CSDE1^{WT}/CSDE1 consensus binding site wild type) (Figure 2G). However, supernatants from infection of CSDE1^{P5S} mutant tumor cells with VSV-IFN-β-P/M (CSDE1 consensus binding site mutant) contained levels of DIP that resembled those seen from infection of CSDE1^{WT} with VSV-IFN-β and CSDE1^{WT} with VSV-IFN-β-CSDE1 (Figure 2G).

Trap and ambush oncolytic virotherapy

Given the reproducible and predictable mutation of *CSDE1^{WT}* to *CSDE1^{C-T}* as tumor cells progressively escape oncolysis by VSV-IFN-β, we hypothesized that there would be a time point at which VSV-IFN-β-P/M should match VSV-IFN-β (CSDE1^{C-T} mutant escape cells ∼/< CSDE1^{WT} wild-type cells), and then eventually outperform it as an oncolytic (CSDE1^{C-T} mutant escape cells >> CSDE1^{WT} wild-type cells) as the proportion of escaping tumor cells with the *CSDE1^{C-T}* mutation increases. To model this *in vitro*, tumor cells were exposed sequentially to infection by VSV-IFN-β or VSV-IFN-β-P/M (Figure 3A). Chronic low MOI exposure of CSDE1^{WT} parental tumor cells exclusively to three doses of VSV-IFN-β-P/M killed ∼3 logs fewer tumor cells over the 21-day period than did exposure exclusively to VSV-IFN-β (Figure 3A). Intervention with VSV-IFN-β at days 7 and 14, or just day 14, post VSV-IFN-β-P/M or (VSV-IFN-β-P/M)x2, respectively, was more cytotoxic than continual VSV-IFN-β-P/M (Figure 3A). These data show that VSV-IFN-β-P/M cannot kill therapeutically valuable levels of parental CSDE1^{WT} cells and that CSDE1^{WT} cells remain the predominant population following exposure to this ESC-selected virus.

As expected, although chronic low MOI exposure of CSDE1^{WT} parental tumor cells exclusively to VSV-IFN-β killed large numbers of cells, it still selected for the emergence of virus-resistant cells characterized by fixing of the CSDE1^{C-T} mutation (Figure 3A), as reported previously.[9,21,31] Intervention with the VSV-IFN-β-P/M at days 7 and 14 post VSV-IFN-β was not significantly more cytotoxic than continual VSV-IFN-β (Figure 3A). However, intervention with the VSV-IFN-β-P/M at day 14 post (VSV-IFN-β)×2 almost completely eradicated tumor cells *in vitro*.

The assay of Figure 3A was repeated using CSDE1^{C-T} mutant tumor cells generated by the 21-day selection protocol described previously[9] as the substrate for viral infection. In this scenario, continual exposure of the CSDE1^{C-T} mutant tumor cells to three consecutive doses of VSV-IFN-β-P/M was the most effective cytotoxic combination (Figure 3B). Intervention with one dose of VSV-IFN-β at day 14, or two doses at days 7 and 14 led to the survival of progressively more cells (Figure 3B). As expected, continual exposure of the CSDE1^{C-T} mutant tumor cells to three consecutive doses of VSV-IFN-β was the least therapeutically effective treatment. Moreover, early intervention with (VSV-IFN-β)×1 + (VSV-IFN-β-P/M)×2 (days 7 and 14) was more therapeutic than late intervention with just a single dose of VSV-IFN-β-P/M following two doses of VSV-IFN-β (Figure 3B).

Based on these *in vitro* data, we tested whether a similar strategy of oncolytic virotherapy-based trap (frontline VSV-IFN-β to drive emergence of CSDE1^{C-T} mutant tumor cells) and ambush (treatment with ESC-adapted VSV-IFN-β-P/M) would also be therapeutically valuable in the context of established tumors growing in immune competent mice (Figure 3C). Using a regimen of three rounds of intratumoral virus injection, with each round consisting of three injections every other day (Figure 3C), 50% of mice bearing 10-day established B16 melanomas were tumor free at day 80 upon treatment with two rounds of VSV-IFN-β (trap) followed by one round of VSV-IFN-β-P/M (ambush) (Figures 3D and 3E). This contrasted with no long-term cures upon treatment with three rounds of VSV-IFN-β, although this treatment was significantly more therapeutic than control PBS treatment (Figures 3D and 3E, $p < 0.0001$). Any treatment regimen initiated with intratumoral injection of VSV-IFN-β-P/M was no more effective than PBS treatment (Figures 3D and 3E).

Successful sequential trap and ambush virotherapy was associated with T cell priming

To assess the immunological consequences of this successful sequential virotherapy regimen, splenocytes from mice treated in Figure 3D and 3E were re-stimulated *in vitro* with MHC class I, H2K^{b}-restricted T cell epitopes from potentially relevant antigens. Splenocytes from control (PBS)-treated mice did not recognize any of the panel of immunogens as measured by IFN-γ release (Figure 4A). Mice treated with three rounds of VSV-IFN-β, a regimen that gave significant therapy but no long-term cures (Figures 3D and 3E), had strong T cell responses against the virus as assessed by IFN-γ secretion in response to the immunodominant VSV N_{52-59} epitope.[32] However, T cell responses against either of the SELF epitopes derived from the CSDE1^{WT} or TYRP2 (melanoma-associated antigen) proteins were equivalent and at background levels. We have previously shown that, in the context of C57BL/6 H2K^{b} mice, the CSDE1^{C-T} mutation, associated with the development of VSV-IFN-β ESC tumor cells, generates a heteroclitic neo-epitope, which primed T cell responses against both itself and, to a lesser extent, against wild-type CSDE1^{WT}.[10,21] Splenocytes from mice treated with three rounds of VSV-IFN-β virotherapy consistently showed a trend toward increased T cell responses against this CSDE1^{P5S}-containing EATA

selected for escape from VSV over 21 days (Hep3B-CSDE1^{C-T} cells) (lanes 4–6) were infected with VSV-IFN-β, VSV-IFN-β-CSDE1, or VSV-IFN-β-P/M (MOI = 3.0). After 6 h viral M protein was measured by western blotting. Representative of two experiments. (G) For defective interfering particle (DIP) assay, target cells (Hep3B or Hep3B-CSDE1^{C-T}) were infected with VSV-IFN-β, VSV-IFN-β-CSDE1, or VSV-IFN-β-P/M (MOI = 3.0) and supernatant was harvested at 72 h. Supernatant was diluted as shown (neat, 1:10, 1:100) and added to a stock VSV-IFN-β used to infect BHK cells (MOI = 20 of VSV stock). Viral titers (pfu/mL) were determined by plaque assay at 24 h. Significance was determined using two-way ANOVA with Tukey's two-way multiple comparisons. Statistical significance was set: *$p < 0.05$, **$p < 0.01$, ***$p < 0.001$, ****$p < 0.0001$.

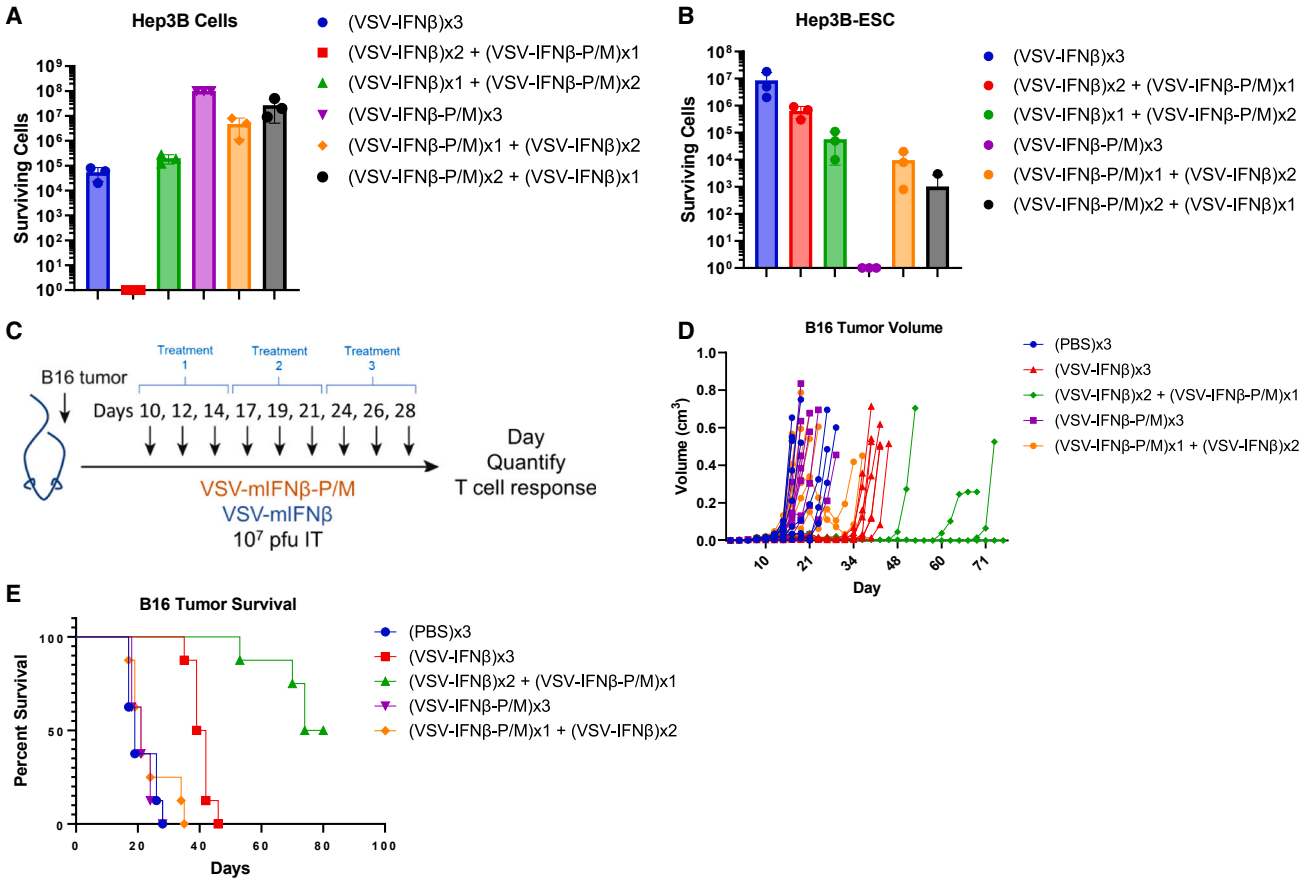

Figure 3. Trap and ambush oncolytic virotherapy

Target cells were infected in triplicate on days 1, 7, and 14 with VSV-IFN-β or VSV-IFN-β-P/M (MOI = 0.01) in the combinations shown, with surviving cells counted at day 21. (A) Parental Hep3B cells, (B) Hep3B-ESC cells, (C) C57BL/6 mice were injected s.c. with B16 tumors on day 1. Starting at day 10, mice were treated intratumorally (i.t.) (10^7 pfu/injection) with either VSV-IFN-β or VSV-IFN-β-P/M for three rounds of treatment. Each round consisted of three injections of a specific virus with the sequence of viruses shown. (D) Tumor volumes of all mice in all groups. (E) Survival of C57BL/6 mice (n = 40 mice, n = 8 per arm) is shown with significance determined using a log rank Mantel-Cox test (Figure S1). Statistical significance was set: *p < 0.05, **p < 0.01, ***p < 0.001, ****p < 0.0001.

peptide (MSFDSNLLH) compared with the CSDE1^{WT} peptide (MSFDPNLLH), although this did not reach significance (Figure 4A)—suggesting that very low levels of T cell priming against the emerging CSDE1^{P5S} epitope were occurring. Splenocytes from mice treated with the therapeutically ineffective regimen of (VSV-IFN-β-P/M)×1 + (VSV-IFN-β)×2 were effectively re-stimulated by the viral VSV N_{52-59} epitope, but had only background levels of activity against the SELF CSDE1^{WT} or TYRP2 epitopes or against the heteroclitic CSDE1^{P5S} epitope (Figure 4A). In contrast, splenocytes from mice treated with the therapeutically optimal regimen of (VSV-IFN-β)×2 + (VSV-IFN-β-P/M)×1 secreted increased amounts of IFN-γ upon re-stimulation *in vitro* with the EATA CSDE1^{P5S} peptide (Figure 4B).

Sequential trap and ambush virotherapy induces immune checkpoint CD200R1

Given the evidence of induction of potentially beneficial T cell responses against tumor- and escape tumor-associated antigens (Figures 4A and 4B), splenocytes and tumors were screened for expression of potential immune checkpoint inhibitors whose expression may be limiting these therapeutic T cell responses *in vivo*. Of several potential T cell immune checkpoint mediators, we observed a highly significant increased expression of CD200R1, an inhibitory/immunosuppressive receptor known to be expressed on monocytes and dendritic cells (Figures 4C and 4D).[33,34] High levels of induced expression of CD200R1 were observed in both splenocytes and whole tumor explants following treatment with the therapeutically most effective treatment of (VSV-IFN-β)×2 + (VSV-IFN-β-P/M)×1 compared with any of the other treatments (Figures 4C and 4D). Therefore, we investigated whether this elevated expression of CD200R1 would provide a potential target for ICB in combination with the sequential oncolytic virotherapy regimen. Thus, splenocytes from mice treated with different rounds of virotherapy were re-stimulated *in vitro* with MHC class I-restricted peptide targets in the presence of the CD200 activation receptor ligand (CD200AR-L) peptide, which we have previously shown to block the inhibitory signaling of

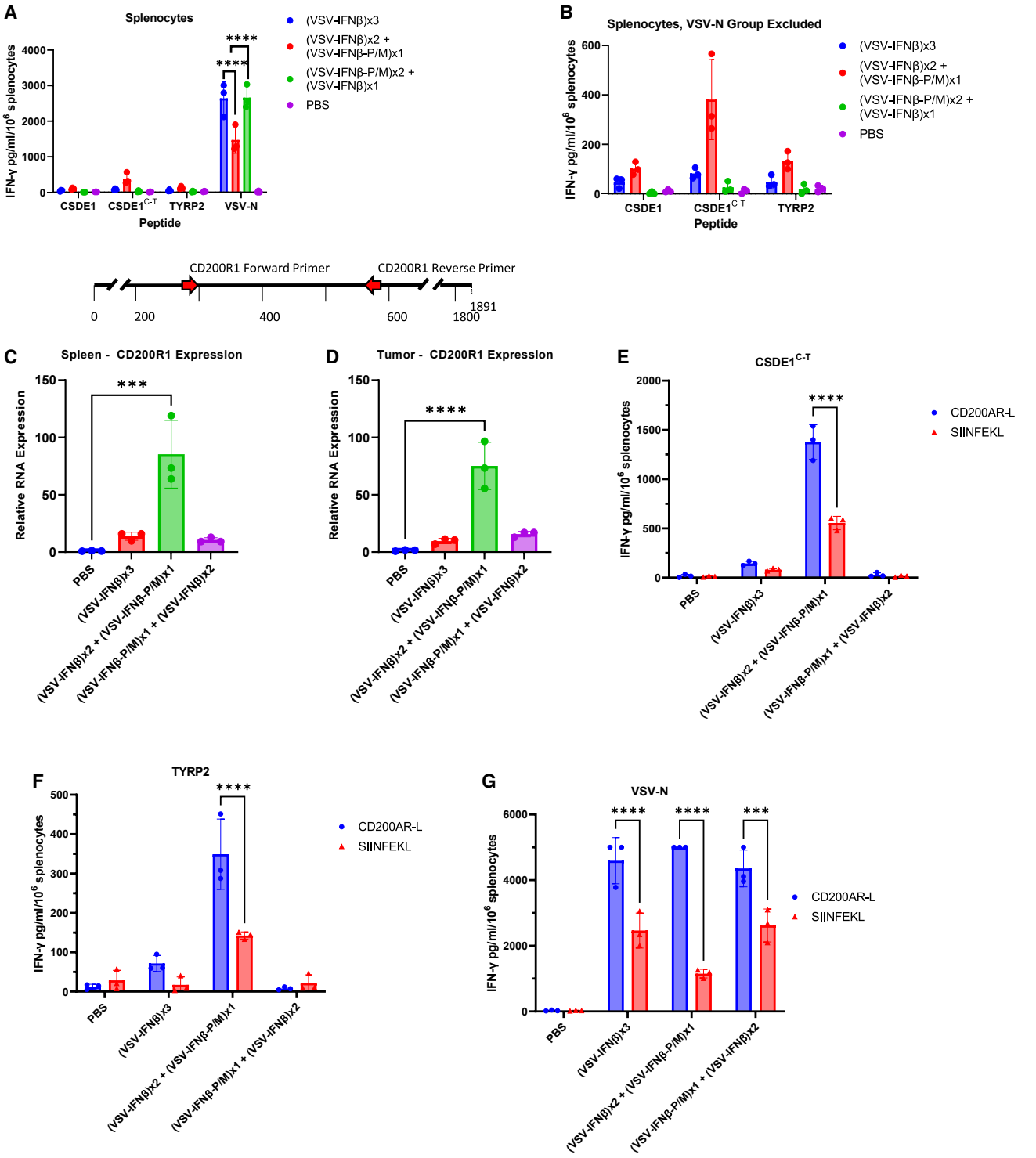

Figure 4. Sequential trap and ambush virotherapy is associated with T cell priming and epitope spreading

Spleens and tumors were harvested from C57BL/6 mice treated as described in Figure 3 at day of sacrifice. (A) Splenocytes from each treatment group were re-stimulated with CSDE1, CSDE1^{P5S}, TYRP2, or VSV-N$_{52-59}$ peptides and IFN-γ measured (pg/mL) via ELISA. (B) Identical to (A) with the exception of the VSV-N group which was removed to clarify smaller-scale changes in IFN-γ. Significance for (A and B) was determined using two-way ANOVA with Tukey's two-way multiple comparisons. (C and D) qRT-PCR levels of *CD200R1* RNA from splenocytes and tumor cells from each treatment group (CD200R1-specific forward and reverse primers). Significance for (C and D)

(legend continued on next page)

CD200R to enhance immunotherapy.[34–39] In the presence of the negative control SIINFEKL peptide, as before, splenocytes from mice treated with the (VSV-IFN-β)×2 + (VSV-IFN-β-P/M)×1 regimen showed significant recall T cell responses against the heteroclitic EATA CSDE1^{P5S}, the B16 melanoma-associated antigen TYRP2, and the immunodominant VSV N_{52-59} viral antigen (Figures 4E–4G). Treatment with (VSV-IFN-β)×3 also induced a low but detectable response to CSDE1^{P5S} (as well as an anti-viral response) but no significant epitope spreading against TYRP2 (Figures 4E–4G). Treatment with the therapeutically ineffective (VSV-IFN-β-P/M)×1 + (VSV-IFN-β)×2 was only able to induce detectable anti-VSV T cell responses. However, the CD200AR-L peptide, added to antagonize CD200R signaling, significantly increased the potency of the Th1 anti-CSDE1^{P5S}, TYRP2, and VSV N_{52-59} T cell responses in mice treated with the effective (VSV-IFN-β)×2 + (VSV-IFN-β-P/M)×1 regimen (Figures 4E–4G). In addition, CD200AR-L also potentiated the anti-VSV T cell response in splenocytes from all treatment groups and showed a consistent, but non-significant, trend to enhance the anti-CSDE1^{P5S} and TYRP2 T cell responses in splenocytes from mice treated with (VSV-IFN-β)×3.

Sequential trap and ambush viro-immunotherapy

Based on these data, we hypothesized that the effective sequential oncolytic virotherapy trap and ambush regimen described in Figures 3D and 3E would be further enhanced by the addition of ICB with the CD200AR-L peptide (Figure 5A). In our model of subcutaneous B16 tumors, treatment with CD200AR-L ICB (starting at day 10 post tumor seeding) had no therapeutic effect (Figures 5A and 5B). In our previous studies, we demonstrated that ICB with anti-PD-1 antibody following VSV virotherapy is most effective when administered late following initiation of the virus.[21] Consistent with this, we observed that the treatment observed with three rounds of (VSV-IFN-β)×3 with control SIINFEKL peptide treatment (Figure 5B) was significantly enhanced by ICB with CD200AR-L initiated at the start of the third cycle of VSV-IFN-β (Figure 5B).

As we have demonstrated previously,[21] the efficacy of (VSV-IFN-β-CSDE1)×3 was more pronounced than (VSV-IFN-β)×3, confirming that additional expression of CSDE1 from the virus generates a significantly better oncolytic (Figure 5B vs. 5C and 5E). As for treatment with (VSV-IFN-β)×3, ICB with CD200AR-L improved survival compared with (VSV-IFN-β-CSDE1)×3 (Figure 5C). Sequential trap and ambush virotherapy with (VSV-IFN-β-CSDE1)×2 + (VSV-IFN-β-P/M)×1 was more therapeutic than our next most effective (VSV-IFN-β-CSDE1)×3 treatment (Figure 5D vs. 5C and 5E), confirming that emergence of VSV-ESC tumors can be treated with the ESC-adapted VSV-IFN-β-P/M. Addition of ICB with CD200AR-L significantly enhanced therapy of this virotherapy trap and ambush still further, confirming that the anti-tumor effects are mediated in part by immune effectors, the activity of which can be enhanced *in vivo* by ICB (Figures 5D and 5E).

DISCUSSION

In multiple models of oncolytic virotherapy, it is common to see an early anti-tumor response followed by aggressive escape and tumor recurrence.[1–15,31,40–44] Here, we show that the evolution of viral ESC tumor cells harboring the critical escape-promoting *CSDE1*$^{C\text{-}T}$ mutation can be exploited by a virological ambush using a mutant VSV (VSV-IFN-β-P/M) selected for its ability to replicate to near wild-type levels in CSDE1^{P5S} expressing ESC tumor cells. Sequential killing of primary (VSV-IFN-β-sensitive; VSV-IFN-β-P/M-insensitive) and then emerging escape (VSV-IFN-β-insensitive; VSV-IFN-β-P/M-sensitive) tumor cells with two different oncolytic viruses also facilitated the priming of anti-tumor T cells responses. These T cell responses could be further exploited to convert a tumor model completely insensitive to ICB to one in which the combination of oncolytic virotherapy with ICB could cure >80% of mice with established tumors.

In our previous work,[21] we showed tumors that escape initial VSV oncolytic therapy can be targeted using an immunological trap and ambush. Thus, oncolytic VSV virotherapy forces tumor cells to evolve a specific immunogenic mutation (CSDE1^{P5S}) to escape the VSV therapy (the trap). Subsequently, those escaping cells were cleared by a T cell response directed specifically against the enforced CSDE1^{P5S} mutation by expressing the mutated CSDE1^{P5S} protein from VSV (VSV-CSDE1^{C-T}) (the ambush). In addition, the heteroclitic anti-CSDE1^{P5S} T cell response was augmented in its efficacy *in vivo* with ICB with anti-PD-1 therapy directed against the highly antigen-focused high PD-1-expressing anti-CSDE1^{P5S} T cells. In this study, we show that a virological trap and ambush strategy can also be effective at targeting tumors which escape initial VSV oncolysis. In this case, sequential treatment with the escape-adapted VSV-P/M virus allowed the VSV-P/M virus to replicate in the CSDE1^{P5S} escaped cells allowing for robust oncolysis of escape cells. In the current manuscript, the immunological component of anti-tumor therapy (not likely to be focused against a single tumor-associated antigen) was augmented by treatment with the CD200AR-L checkpoint inhibitor targeting highly increased levels of CD200R1 in both splenocytes and whole tumor explants following our successful (VSV-IFN-β)×2 + (VSV-IFN-β-P/M)×1 therapy. Experiments are underway to compare anti-PD-1 and CD200AR-L ICB in combination with both the immunological and virological trap and ambush strategies.

Furthermore, we have shown that frontline treatment with oncolytic VSV-IFN-β induces APOBEC and other mediators of cellular

was determined using one-way ANOVA. (E–G) Splenocytes from each treatment group were re-stimulated with (E) CSDE1^{P5S}, (F) TYRP2, or (G) VSV-N_{52-59} peptides. CD200AR-L, a peptide inhibitor of the CD200/CD200R1interaction, or a control peptide, SIINFEKL, were added to treatment groups and IFN-γ was measured (pg/mL). Significance for (E–G) was determined using two-way ANOVA with Tukey's two-way multiple comparisons. Statistical significance was set: *$p < 0.05$, **$p < 0.01$, ***$p < 0.001$, ****$p < 0.0001$.

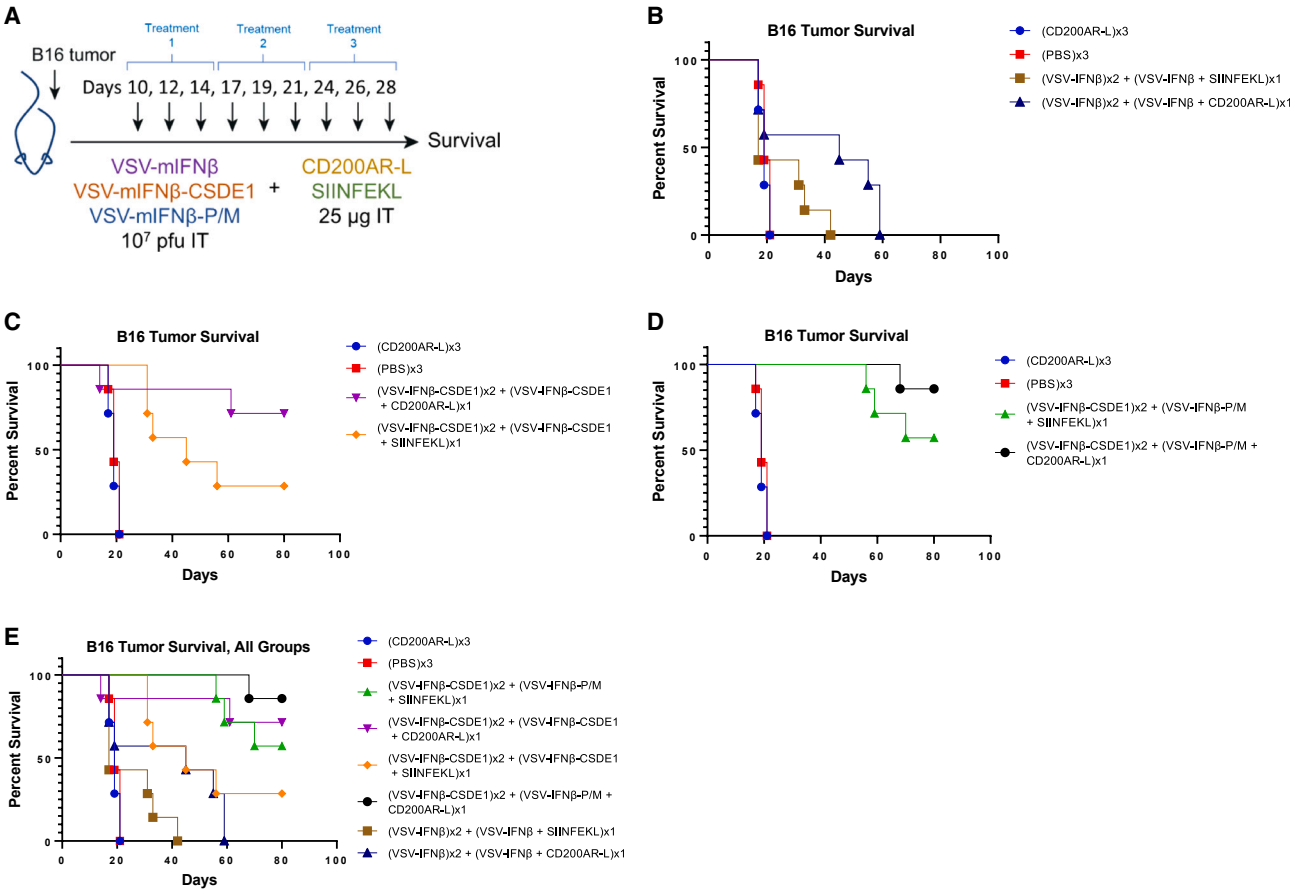

Figure 5. Sequential trap and ambush virotherapy in combination with CD200AR-L immune checkpoint blockade

(A) C57BL/6 mice were injected s.c. with B16 tumors on day 1. Starting at day 10, mice were treated intratumorally (i.t.) (10^7 pfu/injection) with VSV-IFN-β-CSDE1, VSV-IFN-β, or VSV-IFN-β-P/M for three rounds of treatment. Each round consisted of three injections of a specific virus with the sequence of viruses shown. Animals treated with virus and immune checkpoint blockade with CD200AR-L or SIINFEKL peptide were treated with 25 µg peptide per injection 3 times per week only in the last week of treatment. The (CD200AR-L)×3 group received three complete rounds of treatment with CD200AR-L over 3 weeks with three injections per week. (B–D) Survival of individual treatment groups are shown; all the sequential viral therapy arms showed improvement in the number of surviving mice with the addition of CD200AR-L in comparison with the addition of the control peptide SIINFEKL. (E) Overall survival of all groups combined (n = 64 mice, 8 mice per arm) with significance determined using a log rank Mantel-Cox test (Figure S2).

mutation.[9,10,21] This drives the evolution, selection, and fixing, of specific mutations that allow cells to support replication of, and oncolysis by, the virus significantly less efficiently than the wild-type tumor cells. Of several mutations we observed in a range of murine and human tumor cells which evolved to escape VSV-IFN-β oncolysis, the $CSDE1^{P5S}$ mutation occurred at the highest frequency.[9,10,21] We showed that this *C-T* mutation in CSDE1 can generate a heteroclitic neo-epitope in the context of $H2K^b$ MHC class I in the C57BL/6 mouse that could be used to ambush ESC tumor cells by vaccination with the mutant $CSDE1^{P5S}$ expressed within the virus.[21] These data indicated a critical role for the $CSDE1^{WT}$ protein in the replication cycle of VSV. Therefore, we reasoned that the provision of additional levels of $CSDE1^{WT}$ protein by expression of the protein from the virus itself would enhance viral replication and oncolytic activity. In this respect, we show here that exogenous addition of CSDE1 to the VSV-IFN-β virus enhances its titer, oncolytic potency, and ability to reduce tumor cell escape from virotherapy (Figure 1).

Given that $CSDE1^{WT}$ is mutated at very high frequency in VSV-IFN-β-ESC tumor cells, we hypothesized that it would be possible to isolate VSV-IFN-β variants which, given sufficient time and selective pressure, could adapt to the loss of functional $CSDE1^{WT}$ in $CSDE1^{P5S}$ ESC cells. Following repeated passage through $CSDE1^{P5S}$-expressing ESC tumor cells, we isolated a mutant VSV-IFN-β that replicates at near wild-type levels in ESC $CSDE1^{P5S}$ mutant cells. This variant, VSV-IFN-β-P/M, carries a C-U point mutation in the only perfect CSDE1 consensus binding site in the viral genome within the IGR between the viral *P* and *M* genes. This IGR P/M mutation restored the ability of the mutated $CSDE1^{P5S}$ protein to facilitate efficient viral replication in ESC cells, a property that is lost with wild-type virus

growing in CSDE1^{P5S} mutant cells (Figure 1). As a result, the VSV-IFN-β-P/M virus, while very poorly effective against wild-type (non-escaped) tumor cells, is a potent oncolytic against tumor cells that have already escaped from VSV-IFN-β oncolysis (Figure 1).

The data of Figure 2 show that, when the host cell CSDE1 status is matched with the viral P/M IGR status (wild type with wild type or mutant with mutant), viral replication was optimal; however, when host cell wild-type CSDE1 was mismatched with a mutant CSDE1 consensus binding site, or vice versa, viral fitness was greatly reduced. This loss of viral fitness was directly associated with a major block in expression of the viral matrix protein, which in turn generated significantly higher concentrations of DIPs (Figure 2). Further detailed mechanistic studies are currently underway to test the hypothesis that CSDE1^{WT} protein directly binds to the CSDE1 consensus binding site in the P/M IGR of the virus; that this binding is directly disrupted by the CSDE1^{P5S} mutation, which evolves in ESC cells; and that the C-U mutation in the CSDE1 consensus binding site that enables VSV-IFN-β-P/M to replicate well in CSDE1^{P5S} mutant ESC cells restores a direct binding of the mutant CSDE1^{P5S} to the mutated P/M IGR. Our data in Figure 2 show that normal transcription of unicistronic M RNA is restored through complementation of the CSDE1^{P5S} mutant protein in ESC cells by the C-U mutation in the P/M IGR in the VSV-IFN-β-P/M virus. Therefore, we are currently testing the hypothesis that the C-U mutation in the IGR allows the mutated CSDE1^{P5S} protein to bind to the mutated CSDE1 consensus site in the positive strand of the IGR during the last stage of transcription of the *P* gene. Once the mutant CSDE1^{P5S} has bound to the mutated consensus binding site, this interaction allows the viral polymerase to detach from the *P* gene mRNA releasing the unicistronic P mRNA. It may also be that mutant CSDE1^{P5S} binding to the mutated consensus binding site in the positive strand of the IGR allows for reattachment of the polymerase to the viral negative sense genome to initiate transcription of the *M* gene mRNA.

Having identified oncolytic viruses specifically adapted to replication in both primary and escape tumor cells, we went to show that the evolution of viral ESC tumor cells harboring the critical escape-promoting CSDE1^{C-T} mutation can be exploited by a virological trap and ambush strategy. We observed that emergence of a predominantly escape (CSDE1^{C-T} mutant) population from a CSDE1^{WT} population of tumor cells requires between 7 and 14 days at least *in vitro* (Figure 3). Furthermore, this evolution from virus (VSV-IFN-β)-sensitive to virus escape phenotype makes the ESC population highly vulnerable to infection/replication and oncolysis by the ESC-adapted VSV-IFN-β-P/M virus (Figure 3). We were also able to translate these *in vitro* findings into a very effective *in vivo* regimen to treat tumors that otherwise escape frontline VSV-IFN-β treatment (Figure 3). By sequential delivery of a primary tumor-targeting virus (VSV-IFN-β as the trap) followed by an escape targeting oncolytic VSV (VSV-IFN-β-P/M as the ambush) *in vivo* a high proportion of tumors which otherwise escape VSV-IFN-β oncolytic virotherapy could be cured (Figure 3). These data are consistent with a model in which early treatment of CSDE1^{WT} tumors with VSV-IFN-β drove the evolution of escape tumor cells into a CSDE1^{P5S} phenotype (after approximately 2 weeks) that was itself a highly susceptible substrate for subsequent ambush with the ESC-adapted VSV-IFN-β-P/M virus, leading to significant numbers of mice cured of their tumors (Figure 3). Experiments are underway to investigate how the sequential treatment with (VSV-IFN-β)×2 + (VSV-IFN-β-P/M) selects for additional mutations either within, or separate from, the *CSDE1* gene (such as, for example, whether reversion to CSDE1^{WT} is seen in CSDE1^{P5S} mutant tumor cells selected to escape from the VSV-IFN-β-P/M virus). This is distinct from prior work in which VSV therapy alone was able to cure murine tumor models.[31] In this study, we tested the efficacy of a relatively attenuated version of VSV (VSV-IFN-β compared with VSV-GFP) against B16.F10 tumors which are relatively sensitive to type I IFNs compared with other variants of B16 melanomas (such as B16ova). These factors, coupled with lower doses of virus (nine injections of 10^7 pfu of virus compared with six injections of 5×10^8 pfu) and treatment of more established tumors (7-day compared with 10-day), combine to create conditions in which the virus alone was ineffective.

Consistent with a major role of the activation of anti-tumor immune effectors by oncolytic virotherapy,[45–47] the *in vivo* selection of CSDE1^{P5S} mutant cells evolving to evade VSV-IFN-β virotherapy, followed by their lysis by VSV-IFN-β-P/M, was sufficient to prime endogenous T cell responses against the CSDE1^{P5S}-derived MSFDSNLLH heteroclitic neoepitope as well as against the wild-type CSDE1^{WT}-derived MSFDPNLLH peptide (Figure 4A). Optimizing the killing of tumor cells in this way also facilitated the breaking of tolerance to the self melanoma-associated antigen TYRP2 (Figure 4), showing that successful sequential trap and ambush virotherapy was associated with epitope spreading to enable the breaking of tolerance to therapeutically relevant tumor antigens (Figure 4A). Therefore, the most effective sequential trap and ambush oncolytic therapy regimen was associated with the induction of T cell responses with potential therapeutic value to clearing both primary (TYRP2) and ESC (TYRP2 and CSDE1^{P5S}) tumors.

Based on these observations, we tested the hypothesis that these anti-tumor T cell responses could be further enhanced using ICB. By screening tumors and spleens for expression of potential immune checkpoint molecules, we observed that sequential trap and ambush oncolytic virotherapy induced high levels of expression of the immune checkpoint CD200R (Figure 4). CD200 is a type Ia transmembrane glycoprotein in the immunoglobulin supergene family which is closely related to B7 family costimulatory receptors[33] and acts as an inhibitory/immunosuppressive receptor on monocytes and dendritic cells.[33–39] We have previously published data demonstrating this overexpression in the tumor microenvironment and that CD200AR-L administration reactivates antigen-presenting cells and upregulates monocyte differentiation to immature dendritic cells.[39] We confirmed that CD200 was acting as a negative regulator of the anti-tumor T cell response in our model because, at least *in vitro*, blockade of CD200R with the CD200AR-L peptide significantly enhanced anti-tumor T cell responses (Figure 4). We have repeatedly

observed that our model of subcutaneous B16 tumors is completely insensitive to ICB with a variety of ICB strategies, including anti-PD-1, anti-PD-L1, and anti-TIM3,[10,21,48] a finding that was repeated here with CD200AR-L ICB (starting at day 10 post tumor seeding) (Figures 5A and 5B). We have observed previously with combination VSV and anti-PD-1 viro-immunotherapy that only late administration of the ICB (at least 7 days post virus) significantly enhanced therapy of virus alone.[21] Consistent with those findings, treatment with three rounds of (VSV-IFN-β)×3 was significantly enhanced by ICB with CD200AR-L initiated at the start of the third cycle of VSV-IFN-β (Figure 5B). As a means to optimize the initial round of oncolysis, we confirmed the findings of Figure 3 that the efficacy of (VSV-IFN-β-CSDE1)×3 was significantly better than (VSV-IFN-β)×3 (Figure 5B vs. 5C and 5E) and observed that ICB with CD200AR-L also significantly added to the therapeutic value of direct oncolysis by this improved VSV (Figure 5C). Optimal sequential trap and ambush virotherapy with (VSV-IFN-β-CSDE1)×2 + (VSV-IFN-β-P/M)×1 was significantly more therapeutic than (VSV-IFN-β-CSDE1)×3 (Figure 5D vs. 5C and 5E), confirming that emergence of VSV-ESC tumors can be treated with the ESC-adapted VSV-IFN-β-P/M. Finally, combination of ICB with CD200AR-L significantly enhanced therapy of this virotherapy trap and ambush still further (Figures 5D and 5E). Further detailed investigation of the tumor microenvironment and the changes in it induced by these sequential viruses will elucidate exactly which immune/tumor cells are induced to express the CD200R checkpoint molecule and which immune effectors mediate the enhanced therapy associated with CD200AR-L ICB in this model. Therefore, we have shown that the generation of anti-tumor T cell responses by sequential trap and ambush virotherapy can be further exploited using ICB to convert a tumor model completely insensitive to ICB to one in which the combination of oncolytic virotherapy with ICB could cure >80% of mice with established tumors.

We are currently testing the hypothesis that CSDE1^{P5S}-mutated VSV-escape tumor cells will inevitably evolve additional mutations that allow them to escape replication/oncolysis by the VSV-IFN-β-P/M virus. In addition, if we observe escape *in vitro* we will also select additional VSV which can themselves evolve to replicate in these VSV-IFN-β-P/M escaped cells.

In summary, we show here that the emergence of tumors which escape frontline oncolytic virotherapy is characterized by reproducible and predictable genetic mutations that confer the escape phenotype. However, given sufficient time and selective pressure, viral variants can also be isolated, which adapt extremely well to these escape phenotypes. We exploited this phenomenon of dual tumor and viral evolution to develop a virological trap and ambush therapy. In this scenario, frontline treatment with a virus able to replicate well in primary tumors is used sequentially with a virus specifically adapted to the cellular genotype/phenotype induced by escape from that virus. This sequential treatment was highly effective at treating tumors that otherwise escaped frontline therapy. Our data also show that trap and ambush virotherapy using sequential administration of oncolytic viruses specifically adapted to both primary and escape tumors induced anti-tumor T cell immune responses that confer significant sensitivity to ICB upon an otherwise ICB-insensitive tumor model. Viruses of many different types have a well-documented ability to evolve and adapt to replication environments induced within (tumor) cells by almost any stimulus. We propose that it will be possible to select viruses tailored specifically to replicate well in tumor cells carrying reproducible and predictable genotypes/phenotypes associated with escape from many different forms of frontline therapy (chemotherapy, radiation therapy, ICB therapy, oncolytic virotherapy). Therefore, our findings here are significant in that they offer the possibility to develop highly specific viruses for use as escape-targeting oncolytic viro-immunotherapeutic agents to be used in conjunction with recurrence of tumors following defined frontline therapies.

MATERIALS AND METHODS

Cell lines and viruses

B16 murine melanoma, human Hep3B hepatocellular carcinoma and BHK cells were originally obtained from American Type Culture Collection (ATCC). Cells were grown in Dulbecco's modified Eagle's medium (HyClone, Logan, UT) + 10% fetal bovine serum (FBS) (Life Technologies). Cell lines were authenticated by morphology, growth characteristics, PCR for tissue-specific gene expression (gp100, TYRP-1, and TYRP-2) and biologic behavior, tested mycoplasma-free (MycoAlert Mycoplasma Detection Kit, Lonza), and frozen. Cells were cultured for <3 months after thawing.

VSV expressing murine IFN-β (VSV-mIFN-β), murine CSDE1^{WT}, murine CSDE1^{C-T}, or green fluorescent protein (VSV-GFP) was rescued from the pXN2 cDNA plasmid using the established reverse genetics system in BHK cells as described previously.[12,15,41] In brief, BHK cells are infected with MVA-T7 at an MOI of 1. Cells are incubated at 37°C and 5% CO_2. After 1 h, cells are transfected with pVSV-XN2 genomic VSV plasmid (10 μg), pBluescript (pBS)-encoding VSV-N (3 μg), pBS-encoding VSV_P (5 μg), and pBS-encoding VSV L proteins (1 μg) using Fugene6 according to the manufacturer's recommendations. Cells were incubated at 37°C and 5% CO_2 for 48 h. After 48 h, supernatant was collected and clarified by passing through a 0.2-μm filter. All transgenes were inserted between viral G and L genes using the XhoI and NheI restriction sites. VSV co-expressing murine IFN-β and CSDE1^{WT} or CSDE1^{C-T} were also generated by cloning the CSDE1 genes between the viral M and G genes. Virus titers were determined by plaque assay on BHK cells or on the stated cell lines in the text.

Mice

Female C57BL/6 (stock 000664) mice were obtained from The Jackson Laboratory. All mice were obtained at 4–8 weeks of age and maintained in a specific pathogen-free BSL2 biohazard facility. Experimental mice were co-housed and exposed to a 12:12-h light-dark cycle with unrestricted access to water and food. The ambient temperature was restricted to 68°F to 79°F and the room humidity ranged from 30% to 70%. All animal studies were conducted in accordance

with and approved by the Institutional Animal Care and Use Committee at Mayo Clinic.

In vitro plaque/survival assays

Hep3B cells were infected in triplicate with VSV-IFN-β, VSV-IFN-β-CSDE1, or VSV-IFN-β-P/M (MOI = 0.1) with viral titers (pfu/mL) were determined in BHK cells by plaque assay at 24, 48, and 72 h. Surviving cells were counted 72 h. For generation of Hep3B-ESC cells, Hep3B tumor cells were exposed to low MOI with VSV-IFN-β, VSV-IFN-β-CSDE1, or VSV-IFN-β-P/M (MOI = 0.01) for 21 days and surviving ESC cells were counted.

In vitro selection of virus-resistant populations

Hep3B cells were infected for 1 h with VSV at an MOI of 0.01. Cells were washed with PBS to remove any excess virus and then incubated for 7 days. Cells were washed every 2 days to remove any dead or floating cells. After 7 days, the cells were collected and re-plated. These cells were subjected to two repeated rounds of infection and re-plating as just described. After 21 days, three total rounds of infection, the remaining virus-escaped cells were collected.

Immunofluorescence

Uninfected B16 parental and B16 parental cells infected with VSV-IFN-β (MOI = 0.1) for 8 h, then seeded in chamber slides (Thermo Fisher Scientific, cat. no. 154534) at 20,000 cells per well. Cells were allowed to attach overnight, then medium was removed, cell monolayer washed once with PBS, then fixed for 20 min (BD Biosciences, cat. no. 555028). Cells were then permeabilized and blocked for 1 h using BD Cytoperm solution. Polyclonal anti-CSDE1 antibody (Atlas Antibodies, cat. no. HPA052221) treatment was done overnight (∼14 h) in humidity chambers to prevent drying. Slides were washed three times with PBS and then incubated with species-appropriate Alexa Fluor 594-IgG (H + L) (Jackson ImmunoResearch, cat. no. 711-586-152) for 60 min in the presence of DAPI. Cells were then observed with a Zeiss LSM 780 confocal laser scanning microscope and the images were analyzed with Zeiss imaging software.

qRT-PCR and sequencing

RNA was prepared using the QIAGEN RNeasy-MiniKit (QIAGEN, Valencia, CA) as per the manufacturer's instructions. One microgram of total RNA was reverse-transcribed in a 20-μL volume using oligo(dT) primers using the First Strand cDNA Synthesis Kit (Roche, Indianapolis, IN). A cDNA equivalent of 1 ng RNA was amplified by PCR with gene-specific primers using glyceraldehyde 3-phosphate dehydrogenase (GAPDH) as the loading control (mgapdh sense: 5′-TCATGACCACAGTCCATGCC-3′; mgapdh antisense: 5′-TCAGCTCTGGGATGACCTTG-3′). qRT-PCR was carried out using a LightCycler480 SYBRGreenI Master kit and a LightCycler480 instrument (Roche) according to the manufacturer's instructions. The ΔΔCT method was used to calculate the fold change in the expression level of viral RNA (P, M, P-M) and GAPDH as an endogenous control for all treated samples relative to an untreated calibrator sample. The following primers were used: P1: 5′-CCTCTCACCA-3′; P2: 3′-GCTCTCAGTT-5′ (120-bp fragment); M1: 5′-GATCTAAGTG-3′; M2: 3′-CATACGAGGC-5′ (120-bp fragment); IGR1: 5′-ACTATGAAAA-3′. CD200R1: 5′ primer: 5′-GCTTTTGGAGAACTTCTGCC-3′; 3′ primer: 5′-CCCAAGCAGCTGGTTTCATT-3′.

Protein expression analysis

Cells were lysed in NP40 lysis buffer containing Pierce Protease inhibitor tablets at a final concentration of 1× (Thermo Scientific). Protein lysates were quantified by bicinchonic acid assay according to the manufacturer's instructions (Pierce, Thermo Scientific). Whole tumor cell lysates, recovered from mice *in vivo*, were normalized by protein concentration prior to ELISA determination (OptE1A, BD Biosciences, San Diego, CA), to ensure equal amounts of protein were assayed from tumors of different sizes. For western blot analysis of VSV M (29 kDa), 20 μg protein lysate was run on a 4%–15% SDS-PAGE gel, transferred to PVDF membrane, and blotted with anti-VSV Matrix clone 23H12, a mouse monoclonal antibody (EMD Millipore, Burlington MA, product no. MABF2347), at a dilution of 1/1,000, overnight at 4°C. Membranes were washed with 0.05% Tween 20 PBS and then probed with anti-mouse secondary antibody (1/10,000) in 5% milk. Membranes were developed with chemiluminescent substrate (Thermo Fisher Scientific).

Defective interfering particle assay

Hep3B or Hep3B-CSDE1^{C-T} cells were infected VSV-IFN-β, VSV-IFN-β-CSDE1, or VSV-IFN-β-P/M (MOI = 3.0) and were incubated for 72 h. Supernatant was collected and either left undiluted or diluted 1:10 or 1:100 in serum-free medium. Fresh BHK cells were seeded the day before in triplicate wells and diluted viral supernatants were allowed to adsorb for 1 h. Stock VSV-IFN-β virus was then added at an MOI of 20 and was incubated for 1 h. Cells were then washed 3× in PBS and fresh supernatant was added. Supernatant was collected 24 h after infection and was titered by plaque assay on BHK cells.

In vivo experiments

All *in vivo* studies were approved by the Institutional Animal Care and Use Committee at Mayo Clinic. Mice were challenged subcutaneously with 2×10^5 B16 melanoma cells in 100 μL PBS (HyClone, Logan, UT, USA). Subcutaneous tumors were treated with doses of 10^7 pfu of virus delivered intratumorally in 50 μL of PBS. Tumors were measured using calipers three times per week and mice were euthanized when tumors reached 1.0 cm in diameter. For experiments using ICB with CD200AR-L or SIINFEKL peptide, mice received 25 μg each of CD200AR-L ([acetyl]IVTWQKKKAVSPANMVTFS [amide]); control mice received 25 μg of control SIINFEKL peptide (Mayo Peptide Synthesis Core).

Immune cell activation

Spleens from C57BL/6 mice were immediately excised upon killing. Single-cell suspensions were achieved *in vitro* via mechanical dissociation. Red blood cells were lysed by resuspension in ammonium-chloride-potassium lysis buffer and incubating at room temperature for 2 min. Cells

were resuspended at a concentration of 1×10^6 cells/mL in Iscove's modified Dulbecco's medium (Gibco) supplemented with 5% FBS, 1% penicillin-streptomycin, and 40 μmol/L 2-mercaptoethanol. Splenocytes were restimulated with CSDE1, CSDE1^{P5S}, TYRP2, or VSV-N$_{52-59}$ peptides with or without the addition of CD200AR-L or control SIINFEKL (5 μg/mL). Supernatants were collected and assayed for IFN-γ by enzyme-linked immunosorbent assay (ELISA) as per the manufacturer's instructions (Mouse TNF-α or Mouse IFN-γ ELISA Kit, OptEIA, BD Biosciences).

Statistical analysis

All analysis was performed within GraphPad Prism software (GraphPad). Multiple comparisons were analyzed using one- or two-way analysis of variances with a Tukey's post hoc multi-comparisons test. Survival data were assessed using a log rank Mantel-Cox test. Data are expressed as group mean ± SD unless otherwise stated.

DATA AVAILABILITY STATEMENT

Data not published within this article will be made available by request from any qualified investigator.

SUPPLEMENTAL INFORMATION

Supplemental information can be found online at https://doi.org/10.1016/j.omto.2023.05.006.

ACKNOWLEDGMENTS

The authors thank Toni L. Woltman for expert secretarial assistance. Funding was provided by the National Institutes of Health (CA262994, CA210964, AI170535-01, and 269384-01), The Richard M. Schulze Family Foundation, the Mayo Foundation, the Shannon O'Hara Foundation, Hyundai Hope On Wheels, and a University of Minnesota and Mayo Partnership Award. The salary of J.S. was supported in part by a T32 grant (5 F31 CA271560-02) from the National Institutes of Health.

AUTHOR CONTRIBUTIONS

M.J.W., T.K., M.B., L.R., R.M.D., M.O., A.B., and R.V. contributed to the conception and design of this paper. T.K., J. Tonne, M. Moore, and R.V. contributed to the development of methodology. M.J.W., T.K., J. Tonne, J. Thompson, M. Metko, and M. Moore contributed to acquisition of data. M.J.W., T.K., B.L.K., J.S., C.U., R.M.D., and R.V. contributed to analysis and interpretation of data. M.J.W., T.K., B.L.K., J.S., C.U., J. Tonne, Jill Thomson, M. Metko, M. Moore, M.B., L.R., R.M.D., M.O., A.B., and R.V. contributed to writing, review, and/or revision of the manuscript. This study was supervised by R.V.

DECLARATION OF INTERESTS

The authors declare no competing interests.

REFERENCES

1. Swanton, C., McGranahan, N., Starrett, G.J., and Harris, R.S. (2015). APOBEC enzymes: mutagenic fuel for cancer evolution and heterogeneity. Cancer Discov. *5*, 704–712. https://doi.org/10.1158/2159-8290.CD-15-0344.

2. McGranahan, N., and Swanton, C. (2015). Biological and therapeutic impact of intratumor heterogeneity in cancer evolution. Cancer Cell *27*, 15–26. https://doi.org/10.1016/j.ccell.2014.12.001.

3. Gatenby, R.A., and Brown, J.S. (2020). The evolution and ecology of resistance in cancer therapy. Cold Spring Harb. Perspect. Med. *10*, a040972. https://doi.org/10.1101/cshperspect.a040972.

4. Kottke, T., Boisgerault, N., Diaz, R.M., Donnelly, O., Rommelfanger-Konkol, D., Pulido, J., Thompson, J., Mukhopadhyay, D., Kaspar, R., Coffey, M., et al. (2013). Detecting and targeting tumor relapse by its resistance to innate effectors at early recurrence. Nat. Med. *19*, 1625–1631. https://doi.org/10.1038/nm.3397.

5. Boisgerault, N., Kottke, T., Pulido, J., Thompson, J., Diaz, R.M., Rommelfanger-Konkol, D., Embry, A., Saenz, D., Poeschla, E., Pandha, H., et al. (2013). Functional cloning of recurrence-specific antigens identifies molecular targets to treat tumor relapse. Mol. Ther. *21*, 1507–1516. https://doi.org/10.1038/mt.2013.116.

6. Zaidi, S., Blanchard, M., Shim, K., Ilett, E., Rajani, K., Parrish, C., Boisgerault, N., Kottke, T., Thompson, J., Celis, E., et al. (2015). Mutated BRAF emerges as a major effector of recurrence in a murine melanoma model after treatment with immunomodulatory agents. Mol. Ther. *23*, 845–856. https://doi.org/10.1038/mt.2014.253.

7. Kottke, T., Evgin, L., Shim, K.G., Rommelfanger, D., Boisgerault, N., Zaidi, S., Diaz, R.M., Thompson, J., Ilett, E., Coffey, M., et al. (2017). Subversion of NK-cell and TNF alpha immune surveillance drives tumor recurrence. Cancer Immunol. Res. *5*, 1029–1045. https://doi.org/10.1158/2326-6066.Cir-17-0175.

8. Evgin, L., Huff, A.L., Kottke, T., Thompson, J., Molan, A.M., Driscoll, C.B., Schuelke, M., Shim, K.G., Wongthida, P., Ilett, E.J., et al. (2019). Suboptimal T-cell therapy drives a tumor cell mutator phenotype that promotes escape from first-line treatment. Cancer Immunol. Res. *7*, 828–840. https://doi.org/10.1158/2326-6066.CIR-18-0013.

9. Huff, A.L., Wongthida, P., Kottke, T., Thompson, J.M., Driscoll, C.B., Schuelke, M., Shim, K.G., Harris, R.S., Molan, A., Pulido, J.S., et al. (2018). APOBEC3 mediates resistance to oncolytic viral therapy. Mol. Ther. Oncolytics *11*, 1–13. https://doi.org/10.1016/j.omto.2018.08.003.

10. Driscoll, C.B., Schuelke, M.R., Kottke, T., Thompson, J.M., Wongthida, P., Tonne, J.M., Huff, A.L., Miller, A., Shim, K.G., Molan, A., et al. (2020). APOBEC3B-mediated corruption of the tumor cell immunopeptidome induces heteroclitic neoepitopes for cancer immunotherapy. Nat. Commun. *11*, 790. https://doi.org/10.1038/s41467-020-14568-7.

11. Kaluza, K.M., Thompson, J.M., Kottke, T.J., Flynn Gilmer, H.C., Knutson, D.L., and Vile, R.G. (2012). Adoptive T cell therapy promotes the emergence of genomically altered tumor escape variants. Int. J. Cancer *131*, 844–854. https://doi.org/10.1002/ijc.26447.

12. Obuchi, M., Fernandez, M., and Barber, G.N. (2003). Development of recombinant vesicular stomatitis viruses that exploit defects in host defense to augment specific oncolytic activity. J. Virol. *77*, 8843–8856. https://doi.org/10.1128/jvi.77.16.8843-8856.2003.

13. Stojdl, D.F., Lichty, B., Knowles, S., Marius, R., Atkins, H., Sonenberg, N., and Bell, J.C. (2000). Exploiting tumor-specific defects in the interferon pathway with a previously unknown oncolytic virus. Nat. Med. *6*, 821–825. https://doi.org/10.1038/77558.

14. Stojdl, D.F., Lichty, B.D., tenOever, B.R., Paterson, J.M., Power, A.T., Knowles, S., Marius, R., Reynard, J., Poliquin, L., Atkins, H., et al. (2003). VSV strains with defects in their ability to shutdown innate immunity are potent systemic anti-cancer agents. Cancer Cell *4*, 263–275. https://doi.org/10.1016/s1535-6108(03)00241-1.

15. Willmon, C.L., Saloura, V., Fridlender, Z.G., Wongthida, P., Diaz, R.M., Thompson, J., Kottke, T., Federspiel, M., Barber, G., Albelda, S.M., and Vile, R.G. (2009). Expression of IFN-beta enhances both efficacy and safety of oncolytic vesicular stomatitis virus for therapy of mesothelioma. Cancer Res. *69*, 7713–7720. https://doi.org/10.1158/0008-5472.CAN-09-1013.

16. Jenks, N., Myers, R., Greiner, S.M., Thompson, J., Mader, E.K., Greenslade, A., Griesmann, G.E., Federspiel, M.J., Rakela, J., Borad, M.J., et al. (2010). Safety studies on intrahepatic or intratumoral injection of oncolytic vesicular stomatitis virus expressing interferon-beta in rodents and nonhuman primates. Hum. Gene Ther. *21*, 451–462. https://doi.org/10.1089/hum.2009.111.

17. Mihailovich, M., Militti, C., Gabaldón, T., and Gebauer, F. (2010). Eukaryotic cold shock domain proteins: highly versatile regulators of gene expression. Bioessays. *32*, 109–118. https://doi.org/10.1002/bies.200900122.

18. Wurth, L., Papasaikas, P., Olmeda, D., Bley, N., Calvo, G.T., Guerrero, S., Cerezo-Wallis, D., Martinez-Useros, J., García-Fernández, M., Hüttelmaier, S., et al. (2016). UNR/CSDE1 drives a post-transcriptional program to promote melanoma invasion and metastasis. Cancer Cell *30*, 694–707. https://doi.org/10.1016/j.ccell.2016.10.004.

19. Guo, A.X., Cui, J.J., Wang, L.Y., and Yin, J.Y. (2020). The role of CSDE1 in translational reprogramming and human diseases. Cell Commun. Signal. *18*, 14. https://doi.org/10.1186/s12964-019-0496-2.

20. Burns, M.B., Lackey, L., Carpenter, M.A., Rathore, A., Land, A.M., Leonard, B., Refsland, E.W., Kotandeniya, D., Tretyakova, N., Nikas, J.B., et al. (2013). APOBEC3B is an enzymatic source of mutation in breast cancer. Nature *494*, 366–370. https://doi.org/10.1038/nature11881.

21. Kottke, T., Tonne, J., Evgin, L., Driscoll, C.B., van Vloten, J., Jennings, V.A., Huff, A.L., Zell, B., Thompson, J.M., Wongthida, P., et al. (2021). Oncolytic virotherapy induced CSDE1 neo-antigenesis restricts VSV replication but can be targeted by immunotherapy. Nat. Commun. *12*, 1930. https://doi.org/10.1038/s41467-021-22115-1.

22. Muto, M., Kamitani, W., Sakai, M., Hirano, M., Kobayashi, S., Kariwa, H., and Yoshii, K. (2018). Identification and analysis of host proteins that interact with the 3'-untranslated region of tick-borne encephalitis virus genomic RNA. Virus Res. *249*, 52–56. https://doi.org/10.1016/j.virusres.2018.03.006.

23. Ju Lee, H., Bartsch, D., Xiao, C., Guerrero, S., Ahuja, G., Schindler, C., Moresco, J.J., Yates, J.R., 3rd, Gebauer, F., Bazzi, H., et al. (2017). A post-transcriptional program coordinated by CSDE1 prevents intrinsic neural differentiation of human embryonic stem cells. Nat. Commun. *8*, 1456. https://doi.org/10.1038/s41467-017-01744-5.

24. Rambow, F., Malek, O., Geffrotin, C., Leplat, J.J., Bouet, S., Piton, G., Hugot, K., Bevilacqua, C., Horak, V., and Vincent-Naulleau, S. (2008). Identification of differentially expressed genes in spontaneously regressing melanoma using the MeLiM swine model. Pigment Cell Melanoma Res. *21*, 147–161. https://doi.org/10.1111/j.1755-148X.2008.00442.x.

25. Martinez-Useros, J., Garcia-Carbonero, N., Li, W., Fernandez-Aceñero, M.J., Cristobal, I., Rincon, R., Rodriguez-Remirez, M., Borrero-Palacios, A., and Garcia-Foncillas, J. (2019). UNR/CSDE1 expression is critical to maintain invasive phenotype of colorectal cancer through regulation of c-MYC and epithelial-to-mesenchymal transition. J. Clin. Med. *8*, 560. https://doi.org/10.3390/jcm8040560.

26. Triqueneaux, G., Velten, M., Franzon, P., Dautry, F., and Jacquemin-Sablon, H. (1999). RNA binding specificity of Unr, a protein with five cold shock domains. Nucleic Acids Res. *27*, 1926–1934. https://doi.org/10.1093/nar/27.8.1926.

27. Heinrich, B.S., Cureton, D.K., Rahmeh, A.A., and Whelan, S.P.J. (2010). Protein expression redirects vesicular stomatitis virus RNA synthesis to cytoplasmic inclusions. Plos Pathog. *6*, e1000958. https://doi.org/10.1371/journal.ppat.1000958.

28. Lahaye, X., Vidy, A., Pomier, C., Obiang, L., Harper, F., Gaudin, Y., and Blondel, D. (2009). Functional characterization of Negri bodies (NBs) in rabies virus-infected cells: evidence that NBs are sites of viral transcription and replication. J. Virol. *83*, 7948–7958. https://doi.org/10.1128/JVI.00554-09.

29. Hoenen, T., Shabman, R.S., Groseth, A., Herwig, A., Weber, M., Schudt, G., Dolnik, O., Basler, C.F., Becker, S., and Feldmann, H. (2012). Inclusion bodies are a site of ebolavirus replication. J. Virol. *86*, 11779–11788. https://doi.org/10.1128/JVI.01525-12.

30. Tawara, J.T., Goodman, J.R., Imagawa, D., and Adams, J.M. (1961). Fine structure of cellular inclusions in experimental measles. Virology *14*, 410–416. https://doi.org/10.1016/0042-6822(61)90332-4.

31. Wongthida, P., Diaz, R.M., Galivo, F., Kottke, T., Thompson, J., Melcher, A., and Vile, R. (2011). VSV oncolytic virotherapy in the B16 model depends upon intact MyD88 signaling. Mol. Ther. *19*, 150–158. https://doi.org/10.1038/mt.2010.225.

32. Obar, J.J., Khanna, K.M., and Lefrançois, L. (2008). Endogenous naive CD8+ T cell precursor frequency regulates primary and memory responses to infection. Immunity *28*, 859–869. https://doi.org/10.1016/j.immuni.2008.04.010.

33. Kotwica-Mojzych, K., Jodlowska-Jedrych, B., and Mojzych, M. (2021). CD200:CD200R interactions and their importance in immunoregulation. Int. J. Mol. Sci. 22. https://doi.org/10.3390/ijms22041602.

34. Moertel, C., Martinez-Puerta, F., Pluhar, G.G.E., Castro, M.G., and Olin, M. (2022). CD200AR-L: mechanism of action and preclinical and clinical insights for treating high-grade brain tumors. Expert Opin. Investig. Drugs *31*, 875–879. https://doi.org/10.1080/13543784.2022.2108588.

35. Mahadevan, D., Lanasa, M.C., Farber, C., Pandey, M., Whelden, M., Faas, S.J., Ulery, T., Kukreja, A., Li, L., Bedrosian, C.L., et al. (2019). Phase I study of samalizumab in chronic lymphocytic leukemia and multiple myeloma: blockade of the immune checkpoint CD200. J. Immunother. Cancer *7*, 227. https://doi.org/10.1186/s40425-019-0710-1.

36. Xiong, Z., Ampudia-Mesias, E., Shaver, R., Horbinski, C.M., Moertel, C.L., and Olin, M.R. (2016). Tumor-derived vaccines containing CD200 inhibit immune activation: implications for immunotherapy. Immunotherapy *8*, 1059–1071. https://doi.org/10.2217/imt-2016-0033.

37. Moertel, C.L., Xia, J., LaRue, R., Waldron, N.N., Andersen, B.M., Prins, R.M., Okada, H., Donson, A.M., Foreman, N.K., Hunt, M.A., et al. (2014). CD200 in CNS tumor-induced immunosuppression: the role for CD200 pathway blockade in targeted immunotherapy. J. Immunother. Cancer *2*, 46. https://doi.org/10.1186/s40425-014-0046-9.

38. Olin, M.R., Ampudia-Mesias, E., Pennell, C.A., Sarver, A., Chen, C.C., Moertel, C.L., Hunt, M.A., and Pluhar, G.E. (2019). Treatment combining CD200 immune checkpoint inhibitor and tumor-lysate vaccination after surgery for pet dogs with high-grade glioma. Cancers (Basel) *11*, 137. https://doi.org/10.3390/cancers11020137.

39. Ampudia-Mesias, E., Puerta-Martinez, F., Bridges, M., Zellmer, D., Janeiro, A., Strokes, M., Sham, Y.Y., Taher, A., Castro, M.G., Moertel, C.L., et al. (2021). CD200 immune-checkpoint peptide elicits an anti-glioma response through the DAP10 signaling pathway. Neurotherapeutics *18*, 1980–1994. https://doi.org/10.1007/s13311-021-01038-1.

40. Stanková, K., Brown, J.S., Dalton, W.S., and Gatenby, R.A. (2019). Optimizing cancer treatment using game theory: a review. JAMA Oncol. *5*, 96–103. https://doi.org/10.1001/jamaoncol.2018.3395.

41. Diaz, R.M., Galivo, F., Kottke, T., Wongthida, P., Qiao, J., Thompson, J., Valdes, M., Barber, G., and Vile, R.G. (2007). Oncolytic immunovirotherapy for melanoma using vesicular stomatitis virus. Cancer Res. *67*, 2840–2848. https://doi.org/10.1158/0008-5472.CAN-06-3974.

42. Galivo, F., Diaz, R.M., Wongthida, P., Thompson, J., Kottke, T., Barber, G., Melcher, A., and Vile, R. (2010). Single-cycle viral gene expression, rather than progressive replication and oncolysis, is required for VSV therapy of B16 melanoma. Gene Ther. *17*, 158–170. https://doi.org/10.1038/gt.2009.161.

43. Willmon, C., Diaz, R.M., Wongthida, P., Galivo, F., Kottke, T., Thompson, J., Albelda, S., Harrington, K., Melcher, A., and Vile, R. (2011). Vesicular stomatitis virus-induced immune suppressor cells generate antagonism between intratumoral oncolytic virus and cyclophosphamide. Mol. Ther. *19*, 140–149. https://doi.org/10.1038/mt.2010.224.

44. Wongthida, P., Diaz, R.M., Galivo, F., Kottke, T., Thompson, J., Pulido, J., Pavelko, K., Pease, L., Melcher, A., and Vile, R. (2010). Type III IFN interleukin-28 mediates the antitumor efficacy of oncolytic virus VSV in immune-competent mouse models of cancer. Cancer Res. *70*, 4539–4549. https://doi.org/10.1158/0008-5472.CAN-09-4658.

45. Melcher, A., Harrington, K., and Vile, R. (2021). Oncolytic virotherapy as immunotherapy. Science *374*, 1325–1326. https://doi.org/10.1126/science.abk3436.

46. Ribas, A., Dummer, R., Puzanov, I., VanderWalde, A., Andtbacka, R.H.I., Michielin, O., Olszanski, A.J., Malvehy, J., Cebon, J., Fernandez, E., et al. (2018). Oncolytic virotherapy promotes intratumoral T cell infiltration and improves anti-PD-1 immunotherapy. Cell *174*, 1031–1032. https://doi.org/10.1016/j.cell.2018.07.035.

47. Melcher, A., Parato, K., Rooney, C.M., and Bell, J.C. (2011). Thunder and lightning: immunotherapy and oncolytic viruses collide. Mol. Ther. *19*, 1008–1016. https://doi.org/10.1038/mt.2011.65.

48. Shim, K.G., Zaidi, S., Thompson, J., Kottke, T., Evgin, L., Rajani, K.R., Schuelke, M., Driscoll, C.B., Huff, A., Pulido, J.S., and Vile, R.G. (2017). Inhibitory receptors induced by VSV viroimmunotherapy are not necessarily targets for improving treatment efficacy. Mol. Ther. *25*, 962–975. https://doi.org/10.1016/j.ymthe.2017.01.023.